The Activity of *Escherichia coli* Dihydroorotate Dehydrogenase Is Dependent on a Conserved Loop Identified by Sequence Homology, Mutagenesis, and Limited Proteolysis†

Olof Björnberg,‡ Anne-Charlotte Grüner,‡,|| Peter Roepstorff,§ and Kaj Frank Jensen*,‡

Center for Enzyme Research, Institute of Molecular Biology, University of Copenhagen, Copenhagen, Denmark and Department of Molecular Biology, Odense University, Odense, Denmark

Received October 1, 1998; Revised Manuscript Received December 15, 1998

ABSTRACT: Dihydroorotate dehydrogenase catalyzes the oxidation of dihydroorotate to orotate. The enzyme from *Escherichia coli* was overproduced and characterized in comparison with the dimeric *Lactococcus lactis* A enzyme, whose structure is known. The two enzymes represent two distinct evolutionary families of dihydroorotate dehydrogenases, but sedimentation in sucrose gradients suggests a dimeric structure also of the *E. coli* enzyme. Product inhibition showed that the *E. coli* enzyme, in contrast to the *L. lactis* enzyme, has separate binding sites for dihydroorotate and the electron acceptor. Trypsin readily cleaved the *E. coli* enzyme into two fragments of 182 and 154 residues, respectively. Cleavage reduced the activity more than 100-fold but left other molecular properties, including the heat stability, intact. The trypsin cleavage site, at R182, is positioned in a conserved region that, in the *L. lactis* enzyme, forms a loop where a cysteine residue is very critical for activity. In the corresponding position, the enzyme from *E. coli* has a serine residue. Mutagenesis of this residue (S175) to alanine or cysteine reduced the activities 10000- and 500-fold, respectively. The S175C mutant was also defective with respect to substrate and product binding. Structural and mechanistic differences between the two different families of dihydroorotate dehydrogenase are discussed.

The enzyme dihydroorotate dehydrogenase (DHOD)[1] uses FMN to catalyze the oxidation of dihydrorotate (DHO) to orotate, the first aromatic intermediate in the biosynthetic pathway toward pyrimidine nucleotides. The reducing equivalents obtained in the first half-reaction, two hydrogen atoms with their electrons, are transferred in the second half-reaction to an electron acceptor, whose nature varies between enzymes of different biological origin. On the basis of sequence similarity, the DHODs can be divided in two major families, i.e., family 1 and family 2 (*1*, *2*). This division correlates with subcellular location of the proteins as well as their preferences for electron acceptors. Enzymes of family 1, found in Gram-positive bacteria and in the anaerobic yeast *Saccharomyces cerevisiae*, are located in the cytosol (*3*−*5*). They have less than 20% sequence identity with the membrane-bound enzymes of family 2, found in eukaryotes and in some prokaryotes such as the Gram-negative bacteria related to *Escherichia coli.* The eukaryotic family 2 enzymes are located in the inner membrane of mitochondria (*6*) and, in the case of the *E. coli* enzyme, it is associated with the cytoplasmic membrane (*7*). In both cases, the flow of electrons is linked to the respiratory chain via quinones.

The Gram-positive bacterium *Lactococcus lactis* encodes two forms of the enzyme, DHODA and DHODB, which both belong to family 1. DHODA is a homodimer (2 × 34 kDa) containing one FMN per subunit (*3*), and the physiological electron acceptor is probably fumarate (*8*). DHODB is a heterotetramer carrying three cofactors, FMN, FAD, and Fe_2S_2 clusters, and it can use NAD^+ as an electron acceptor (*4*, *8*). The structure of DHODA has been determined both in the ligand-free state (*9*) and in complex with the reaction product orotate (*10*), and by site-directed mutagenesis, we identified some residues important for catalysis (*1*). In particular, exchange of a cysteine residue (C130) to alanine or serine dramatically reduced the activity. The cysteine residue may function as a catalytic base in the oxidation of DHO. It is conserved in family 1 and positioned in a loop that covers the substrate binding site.

As representatives of family 2, the enzyme from bovine liver has been extensively characterized (*11*, *12*), and the human enzyme has recently attracted much interest, because its inhibition probably has immunosupressive effects (*6*, *13*, *14*). The *E. coli* enzyme was studied in this laboratory (*15*) before DHODA and DHODB. By having only FMN and

† This work was supported by grants from the Danish National Research Foundation.

* To whom correspondence should be addressed: Kaj Frank Jensen, Center for Enzyme Research, Institute of Molecular Biology, University of Copenhagen, Sølvgade 83H, 1307 Copenhagen K, Denmark. Phone: +45 35322020. Fax: +45 35322040. E-mail: kfj@mermaid.molbio.ku.dk.

‡ University of Copenhagen.

§ Odense University.

|| Present address: Bio-Medical Parasitology Laboratory, Pasteur Institute, Paris, France.

[1] Abbreviations: DCIP, 2,6-dichloroindophenol; DHO, (*S*)-dihydroorotate; DHOD, dihydroorotate dehydrogenase; DHODA and DHODB, the A and B forms of dihydroorotate dehydrogenase from *Lactococcus lactis*; DTT, dithiothreitol; FMN, flavin mononucleotide; MALDI MS, matrix-assisted laser desorption/ionization mass spectrometry; Q_0, 2,3-dimethoxy-5-methyl-1,4-benzoquinone.

10.1021/bi982352c CCC: $18.00
Published on Web 02/13/1999

L. lactis DHODA -NLSCPNVPGKPQLAY-

E. coli DHOD -NISSPNTPGLRTLQY-

FIGURE 1: Protein sequence alignment. The protein sequences of *E. coli* DHOD (residues 172−186) and *L. lactis* DHODA (residues 127−141) are aligned. The underlined residues form a loop in DHODA which connects a β-strand (β4) and an α-helix (α4). Two residues are bolded in the *E. coli* enzyme: S175, which was mutated, and R182, the trypsin cleavage site (the amide bond between R182 and T183).

one type of subunit (37 kDa), the *E. coli* enzyme is reminiscent of DHODA. In sequence, however, it is clearly more related to the mammalian family 2 enzymes (45% identity with the human enzyme, but less than 20% with DHODA).

In this report we have characterized the *E. coli* enzyme obtained from a new expression system. In a sequence alignment, the conserved cysteine residue of family 1 is replaced by a serine residue in the *E. coli* enzyme (Figure 1). The catalytic role of the cysteine residue seems to have been taken over by a serine residue in family 2, and we show that homologous residues surrounding the serine in the *E. coli* enzyme also form a loop crucial for activity. In other aspects, the two enzymes, DHODA and *E. coli* DHOD, are remarkably different, not only with respect to the preference for electron acceptors. The differences also include the type of Ping-Pong mechanism observed, FMN fluorescence, and protein stability.

MATERIALS AND METHODS

Materials. From Sigma, we obtained DHO, orotate, and the quinonic electron acceptors. Other sources were Amersham, for radioactive orotate; Whatman for DEAE−cellulose (DE52); and Pharmacia, for phenyl-sepharose and the Superose columns. Marker proteins for SDS−PAGE, gel-filtration, and sucrose gradients were purchased from Sigma or Boehringer. *E. coli* orotate phosphoribosyltransferase was prepared according to Poulsen et al. (*16*), and DHODA from *L. lactis* was prepared according to Nielsen et al. (*3*). Poly(ethyleneimine)-impregnated cellulose thin layer plates on plastic sheets (PEI-plates) were made according to the procedure of Randerath and Randerath (*17*).

Instrumentation. Centrifugation during the protein purification was carried out in a refrigerated Sorval centrifuge. The ultracentrifuge (L8-55) was from Beckman. Spectra and assays were recorded in a Zeiss Specord S10 diode-array photometer. The fluorescence emission spectra were recorded with a Perkin-Elmer LS-50B luminescence spectrometer. The mass spectra were acquired in positive linear mode on a Voyager Elite time-of-flight mass spectrometer (PerSeptive Biosystems, Framingham, MA) equipped with delayed extraction (delay time 150 ns). Sinapinic acid (Fluka, Buchs, Switzerland), 20 μg/μL in 40% acetonitrile and 0.1% trifluoroacetic acid, was used as matrix, and the sample prepared by mixing 1 μL of protein or digest solution with 1 μL of matrix solution on the target followed by drying. The spectra were calibrated externally using instrument parameters. The stopped-flow equipment (SX-18MV) was from Applied Photophysics. Differential scanning calorimetry (DSC) experiments were performed on a differential scanning microcalorimeter, MC-2, from MicroCal, Inc., Northampton, MA.

Overexpression of E. coli DHOD. The *pyrD* gene, including its regulatory region, was previously cloned in pBR322. This construct, plasmid pED7, provided a 40-fold higher expression than did the same strain (SØ1240) carrying no plasmid (*15*). To improve expression, we made a new construct. The polymerase chain reaction was used to amplify the *pyrD* coding region including its ribosome binding site. Restriction enzyme sites, *Eco*RI upstream and *Bam*HI downstream of the gene, were also introduced by the PCR primers. Using the restriction sites, the amplified fragment was transferred to the expression vector pUHE23−2, containing the LacI-regulated $T7_{A1/04/03}$ promoter. The resulting plasmid, pAG1, was transformed into the strain, SØ6645 (*araD139*Δ*(ara-leu)7679 galU galK* Δ*(lac)174* Δ*pyrD-(MluI−BssHII::Km*^{r}*)* [F′ *proAB lacI*^{q}*Z*Δ*M15 Tn10*]), partially deleted for the chromosomal *pyrD* gene (*3*). Thereby, clones could be selected both by ampicillin and by complementation of the pyrimidine requirement. The sequence of the cloned PCR fragment was determined by the technique of Sanger *et al.* (*18*) using the Sequenase 2.0 kit (USB, Cleveland, OH). The *pyrD* sequence was identical to the one published by Larsen and Jensen (*15*).

Construction of Active Site Mutants. The plasmid pAG1 was used as template in PCR reactions designed to generate the mutants S175A and S175C. The method employed was the same as that described for the *L. lactis* DHODA gene (*1*). The upstream and downstream primers used in the construction of pAG1 were used as flanking primers. Mutant copies of the gene were reinserted in pUHE23-2, where the entire coding regions of the inserts were confirmed by DNA sequencing.

Purification of Recombinant Enzyme. The strain SØ6645 was freshly transformed with plasmid encoding either the wild-type enzyme (pAG1) or the mutant enzymes. Cells were grown at 37 °C in LB broth supplemented with 0.1 g of ampicillin/L. During overexpression of the mutant enzymes, uracil (20 μg/mL) was also provided. When the culture reached an optical density at 436 nm of 0.7−1.0, it was induced by the addition of isopropyl-β-D-thiogalactoside (IPTG) and growth was allowed to continue overnight. The cells were harvested, and further manipulations were carried out at 4 °C or in an ice bath.

Frozen cells from a 2-L culture were resuspended in 80 mL of extraction buffer (5 mM sodium phosphate, pH 7.0, and 0.25 mM EDTA) and disrupted by ultrasonic treatment. After addition of $MgCl_2$ to 5 mM and Triton-X 100 to 0.2%, the extract was cleared by centrifugation at 13 000 rpm (SS-34) for 1 h. The yellow extract was loaded on a DE-52 column (1.6 × 25 cm) previously equilibrated in extraction buffer. The column was washed with 50 mL of extraction buffer including 0.1% Triton X-100 and 100 mL of 50 mM sodium phosphate, pH 6.2, 0.1 mM EDTA, and 0.1% Triton X-100. Using the last buffer, elution was performed by a 400 mL linear gradient of NaCl from 0 to 0.25 M. Solid ammonium sulfate was added to the pooled fractions (about 100 mL) to give a concentration of 0.9 M. A precipitate was formed, and, after a brief centrifugation (10 min 10 000 rpm), the supernatant was loaded on a phenyl-Sepharose column (1.6 × 20 cm) equilibrated in 50 mM sodium phosphate, pH 7.0, and 0.1 mM EDTA (buffer A) containing 0.9 M ammonium sulfate. The yellow enzyme stuck to the very top (2 cm) of the column. The column was first washed with

Table 1: Comparison of *E. coli* DHOD and DHODA from *L. lactis* with Respect to Substrate Specificity[a]

electron acceptor	Q_0 (20 μM)	DCIP (20 μM)	menadione (20 μM)	decylubiquinone (20 μM)	fumarate (500 μM)	O_2
E. coli DHOD	20 ± 2.6	22 ± 2.6	14.5 ± 0.9	58 ± 7 (1.1[b])	1.1 ± 0.2	1.1 ± 0.2
L. lactis DHODA	24 ± 2.5	22 ± 2.0	9.1 ± 0.7	7.4 ± 0.5 (8.8[b])	23 ± 1.5	7.7 ± 0.5

[a] Activities, expressed as μmol/min/mg, were measured at 25 °C in 0.1 M Tris−HCl, pH 8.0, 100 μM EDTA, 0.1% reduced Triton X-100, and 0.5 mM DHO. The reactions were followed spectrophotometrically by the absorbance of orotate as described in Materials and Methods. Standard deviations refer to at least four assays. [b] Activity recorded without the presence of detergent.

a linear 160 mL gradient of ammonium sulfate (from 0.9 to 0 M) in buffer A and then with two volumes of buffer A. The enzyme was eluted in a sharp peak by 1% Triton X-100 in 5 mM sodium phosphate, pH 7.0. To remove Triton X-100 from the enzyme, it was chromatographed on a second DE-52 column (1.6 × 20 mL) in buffer A. The enzyme was eluted by a 400 mL gradient of NaCl (0−0.3 M) in buffer A. It was then concentrated by the Micro Ultrafiltration system from Amicon and dialyzed against buffer A containing 50% glycerol. The enzyme was stored in a liquid form at −20 °C at concentrations around 10 mg/mL.

Gel Electrophoresis and Protein Blotting. SDS−PAGE was run using a Mini Protean II instrument from BioRad. The spacer and resolving gels contained 4% and 17.5% acrylamide, respectively. The semidry blotting apparatus was from JKA Biotech, Denmark. Transfer of proteins to polyvinylidene difluoride (PVDF) membrane (BioRad) was performed according to standard procedures (*19*), using 48 mM Tris−HCl, 39 mM glycine, 1.3 mM SDS, and 20% ethanol as transfer buffer. Edman degradation was performed on an Applied Biosystems 477A gas-phase sequenator at the Department of Protein Chemistry, Institute of Molecular Biology, University of Copenhagen.

Determination of Enzyme Concentration. The purified enzyme preparations were analyzed with respect to content of FMN. The absorbance of diluted samples ($A_{456} - A_{600} \approx 0.15-0.2$) in 50 mM sodium phosphate, pH 7.0, was recorded before heating (95 °C) for 10 min. After centrifugation of the heated sample for 10 min, the concentration of released FMN was calculated from the absorbance at 445 nm of the supernatant and an extinction coefficient of 12 500 M^{-1} cm^{-1}. The determined concentration of released FMN and the absorbance of the enzyme-bound FMN ($A_{456} - A_{600}$) before heating was used to estimate an extinction coefficient for each enzyme preparation.

Size Analyses. The sedimentation properties of *E. coli* DHOD were investigated by 5−20% sucrose gradients in 50 mM sodium phosphate, pH 7.0, prepared in Ultra-Clear tubes (14 × 89 mm) for the Beckman SW41 rotor. The gradients were made in the absence or presence of Triton X-100 (0.1%). Samples (100 μL in 50 mM sodium phosphate, pH 7.0) containing bovine liver catalase, yeast alcohol dehydrogenase and *E. coli* orotate phosphoribosyltransferase as sedimentation markers, and DHOD were loaded to the top of the gradients. After centrifugation for 20 h at 39 000 rpm, the gradients were tapped from the bottom in fractions of 12 or 24 drops (depending on the presence of Triton X-100 which reduced the volume of the drops). The sedimentation coefficient is directly proportional to the migrated distance relative to that of the reference protein. The corresponding molecular mass was calculated according to the equation of Martin and Ames (*20*): $M_1 = M_2(S_1/S_2)^{1.5}$. M_1 and M_2 are the molecular masses and S_1 and S_2 are the sedimentation coefficients of the unknown protein (1) and the reference protein (2), respectively.

Enzyme Assays. Activities were measured in a standard buffer consisting of 0.1 M Tris−HCl, pH 8.0 (adjusted at room temperature), and 0.1 mM EDTA. The assay temperature was 37 °C, except in the comparison between *E. coli* DHOD and DHODA where 25 °C was employed (Table 1). The concentration of wild-type *E. coli* enzyme was between 1 and 200 nM in the assay mixture (1.0 mL).

In the comparison of DHODA and *E. coli* DHOD, activities were followed by the appearing absorbance of orotate. While using the quinones, we monitored the orotate at the quinone−dihydroquinone isosbestic points that were determined by DTT reduction of the quinone in standard buffer. Menadione reduction was recorded at 278 nm, where orotate has its maximal absorbance (ϵ = 6.70 mM^{-1} cm^{-1} (*11*)), Q_0 at 287 nm (ϵ = 6.08 mM^{-1} cm^{-1}), and decylubiquinone at 293 nm (ϵ = 4.43 mM^{-1} cm^{-1}). For DCIP, an isosbestic point at 297 nm was employed (ϵ = 3.40 mM^{-1} cm^{-1}). If no electron acceptor is added, reducing equivalents are transferred to molecular oxygen, and this reaction was followed at 278 nm (ϵ = 6.70 mM^{-1} cm^{-1}). The absorbance of orotate was also used to follow the reaction with fumarate at 300 nm (ϵ = 2.65 mM^{-1} cm^{-1}). Stock solutions of the electron acceptors were made in H_2O (Q_0, DCIP, and fumarate) or in ethanol (menadione and decylubiquinone). With respect to the ring structure, Q_0 and decylubiquinone are identical to the respiratory quinones, which have 6−10 isoprene units attached to the 6-position. Q_0,which lacks substitution at this position, is very soluble in water. Decylubiquinone has an unbranched chain of 10 carbon atoms at the 6-position and is more soluble than the respiratory quinones. Menadione (a naphthoquinone) is an analogue of the menaquinones but without any isoprene side chain. The blue-colored dye DCIP of high redox potential has been used in almost every study on DHODs. It has little resemblance to the quinones.

Specific activity, apparent K_M values for DHO, and inhibition by orotate were determined by using a mixed electron acceptor system, consisting of 200 μM Q_0 and 45 μM DCIP, in standard buffer (without detergent). Due to rapid redox equilibrium reduced Q_0 is reoxidized by DCIP, whose strong absorbance signal at 600 nm is monitored (ϵ = 20 mM^{-1} cm^{-1}). Furthermore, in the absence of detergent, DCIP is used poorly as a substrate and Q_0 becomes preferentially used as electron acceptor. When measuring specific activity, the concentration of DHO was held constant at 1 mM. To obtain apparent K_M values, the DHO concentration was varied from 0 to 200 μM (0, 10, 20, 50, 100, and 200 μM). The concentration range was extended (up to 500 μM) to obtain K_{is} values for orotate. Mixed electron acceptor systems combining DCIP with another quinone have been widely used in studies of DHODs (*6, 11, 14*). Other

investigators have also studied the effects of varying the quinone substrate in the presence of constant concentrations of DCIP and DHO. This was considered as not reliable for the *E. coli* enzyme because DCIP was a good substrate by itself. Thus, DCIP, with its own strong absorbance signal ($\epsilon = 20\ mM^{-1}\ cm^{-1}$), was chosen as variable electron acceptor, and apparent K_M values were determined in standard buffer with 200 μM DHO and 0.1% reduced Triton X-100. The concentration of DCIP was varied from 10 to 60 μM.

Exchange Reaction. The ability of the enzyme to carry out an exchange of radioactivity between DHO and [6-^{14}C]-orotate was tested at 37 °C in a buffer system (0.1 M sodium phosphate, pH 7.0, and 5 mM glucose) with a reduced concentration of oxygen. To suppress the flow of reducing equivalents to oxygen, glucose oxidase, which consumes molecular oxygen, was included at 0.1 mg/mL. During the oxidation of glucose, H_2O_2 is generated and catalase was therefore included, at 0.02 mg/mL. The efficiency of this buffer, with respect to withdrawal of oxygen, was checked by ensuring at least a 100-fold decrease in the steady-state rate with no electron acceptor added and 1 mM DHO.

The reaction mixture (200 μL) containing 1 mM DHO and 0.2 mM [6-^{14}C]-orotate (1.81 GBq/mmol) was preincubated for 5 min before the reaction was started (37 °C) by addition of enzyme. Aliquots (10 μL) of the reaction mixture were taken out at time points (0, 1, 2, 5, 10, 15, and 30 min), quenched by 2 μL of 97% HCOOH, and applied (2 μL) on a poly(ethyleneimine) (PEI) impregnated thin layer plate. The chromatogram was developed with 0.6 M HCOOH, and the radioactive spots representing DHO ($R_f = 0.57$) and orotate ($R_f = 0.19$) were visualized and counted on an Instant Imager from Packard.

Limited Trypsin Digestion. DHOD at a concentration of 0.6 mg/mL (16 μM) in 0.1 M Tris−HCl, pH 8.0, was subjected to bovine trypsin (Sigma) (10 μg/mL) at room temperature. After 15 min, PMSF, 200 μM, was added, and the samples were stored at 4 °C. Cleavage was verified by SDS−PAGE.

Binding of Orotate. The addition of orotate to *E. coli* DHOD induced a large red-shift of the flavin absorbance, which was used to estimate the binding interaction. The red-shift, i.e., $\Delta(A_{515} - A_{600})$, was used as a measure of the fraction (Y) of enzyme that had bound orotate: $Y = \Delta(A_{515} - A_{600})_{obs}/\Delta(A_{515} - A_{600})_{max}$. The concentration of free orotate could then be calculated according to the equation $[orotate]_{free} = [orotate]_{total} - Y[E]_{total}$, assuming a stoichiometric 1:1 complex between enzyme and orotate.

Bleaching of the Flavin Absorption. Reduction of the enzymes was performed under semi-anaerobic conditions by including glucose oxidase (0.04 mg/mL) in the buffer (0.1 M sodium phosphate, pH 7.0, 5 mM glucose, and 0.1 mM EDTA), which reduced the O_2-dependent turnover about 100-fold. DHO (1 mM) was added, and the bleaching was recorded at 475 nm in the diode-array spectrophotometer or in the stopped-flow apparatus. This wavelength was chosen because DHO induces a red-shift of the flavin absorbance, before reduction, within the dead-time of a stopped-flow experiment (Dr. Bruce Palfey, unpublished observation).

Differential Scanning Calorimetry. The microcalorimeter, MC2, was used according to the instructions from the manufacturer (MicroCal, Inc.). The protein samples were dialyzed against 100 mM sodium phosphate, pH 7.0, at 4 °C. Before loading the protein (at concentrations around 1.0 mg/mL) in the sample cell (1.2 mL), it was degassed and stirred in an evacuated chamber for 5 min. Degassed dialysis buffer was loaded in the reference cell. The scan rate was 1 °C/min, and a pressure of 2 bar of nitrogen was kept over the cells. The calorimetric traces were corrected for the instrumental background by subtracting a scan with buffer in both cells. The program Origin 3.1, also from MicroCal Inc., was used for evaluation of the scans.

Data Treatment. Hyperbolic saturation curves from kinetic and binding experiments were fitted using the program KaleidaGraph (Abelbeck Software) for Macintosh. Standard errors were calculated, and figures were also generated by the program. Some kinetic experiments (see figure legends) were also analyzed by the fitting program of Cleland for PC (*21*). Reactions inhibited by orotate were fitted to noncompetitive inhibition (mixed inhibition), where K_{ii} and K_{is} are the inhibitor constants obtained from the effect of orotate on intercepts and slopes of double reciprocal plots. Molecular masses, discussed in relation to the MALDI MS results, were calculated by the program PAWS from Proteometrics.

RESULTS

Protein Expression and Purification. The expression vector pAG1 gave rise to a much higher level of DHOD than previously seen (*15*), but as a result of the higher expression level most of the enzyme (about 60%) was not bound to membranes, as it is the case in nonoverproducing cells (*7*). Therefore, we avoided the use of membrane-isolation as part of the purification procedure. Instead, we now dissolved all enzyme by addition of Triton X-100 to the crude extract and purified the DHOD by column chromatography on DEAE−cellulose and phenyl-Sepharose, as described in Materials and Methods. The last step of DE52 chromatography in the absence of Triton X-100 was primarily introduced to obtain the enzyme free of detergent for crystallography purposes. The final yields of wild-type and mutant enzymes were typically 20 mg/L of bacterial culture.

The Aggregation State. Attempts to define the aggregation state of the *E. coli* enzyme by gel filtration were made, but the apparent size was dependent on the concentration of the loaded enzyme. On a Superose-6 column, run without detergent, the elution volume corresponded to an $M_r = 900\ 000$. Addition of detergent reduced the apparent size to $M_r = 530\ 000$. In these experiments, we loaded the protein in sufficient amounts (0.8 mg/mL) to allow detection by UV. When lower concentrations of enzyme were loaded on Superose-12 or Sephacryl S-300 columns, lower apparent molecular weights were observed both in the presence and absence of detergent. We then tested the enzyme by centrifugation in sucrose gradients. The sedimentation coefficient and apparent molecular mass of DHOD were calculated relative to the well-defined enzyme yeast alcohol dehydrogenase ($S_{20,w} = 7.61$, $M_r = 150\ 000$) according to the equation of Martin and Ames (*20*). Catalase ($M_r = 250\ 000$) and orotate phosphoribosyltransferase ($M_r = 47\ 000$) were also included for control purposes. Triton X-100 greatly influenced the sedimentation of DHOD (loaded in a concentration of 0.5 mg/mL) in the sucrose gradients (Figure

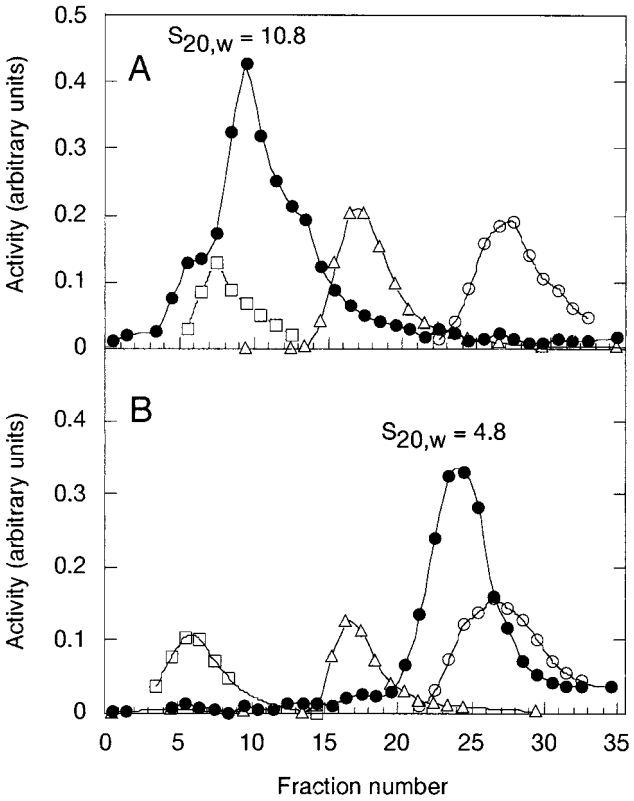

FIGURE 2: Influence of detergent on the sedimentation of DHOD. The direction of sedimentation through the 5−20% sucrose gradients is from right to left. The concentration of DHOD in the applied 100 μL was 0.5 mg/mL. The activities of DHOD (filled circles) and the marker enzymes, bovine liver catalase (squares), yeast alcohol dehydrogenase (triangles), and *E. coli* orotate phosphoribosyltransferase (open circles) are shown. The sedimentation coefficients of DHOD, obtained from the comparison to yeast alcohol dehydrogenase ($S_{20,w} = 7.61$, $M_r = 150\,000$), are indicated. A: Gradient run in the absence of detergent. B: Gradient run in the presence of detergent (0.1% Triton X-100).

2). In contrast, the marker enzymes kept their positions in the gradients. In the absence of detergent, DHOD behaved as large inhomogeneous particles ($M_r = 253\,000$). The presence of detergent reduced the apparent size ($M_r = 75\,500$) and sharpened the activity peak. Two gradients, run in parallel, were analyzed and gave similar results. A lower protein concentration (0.25 mg/mL) of the applied sample did not affect the result. As the molecular mass of the subunit of *E. coli* DHOD is 37 kDa, both according to SDS−PAGE and DNA sequence, the sedimentation behavior in sucrose gradients containing Triton X-100 agrees well with a dimeric structure of the *E. coli* enzyme.

Analysis of the Kinetic Mechanism. Using the mixed electron acceptor system with 200 μM Q_0 and 45 μM DCIP as electron acceptors, we obtained apparent values for V_{max} (about 180 μmol min^{-1} mg^{-1}) and K_M for DHO (28.8 ± 1.5 μM). The apparent K_M value for DCIP, used alone as electron acceptor in the presence of 200 μM DHO, was also about 30 μM (i.e., 30.2 ± 2.2 μM), but the apparent V_{max} (90 ± 5 μmol min^{-1} mg^{-1}) was lower than for the mixed system, because Q_0 is a better electron acceptor than DCIP (see below).

When the concentration of DHO was varied in the presence of different, fixed concentrations of the electron acceptor Q_0, a series of parallel lines were obtained in a

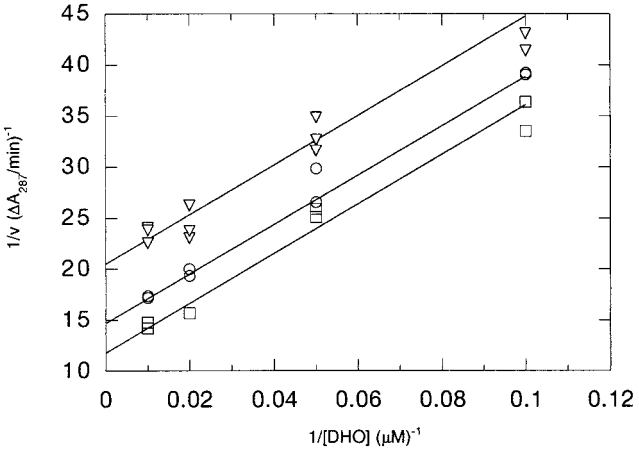

FIGURE 3: Initial velocity pattern varying DHO and Q_0. The concentration of DHO was varied at three fixed concentrations of Q_0: 30 μM (triangles), 60 μM (circles), and 120 μM (squares). The experiment was carried out in standard buffer (0.1 M Tris−HCl, pH 8.0, and 0.1 mM EDTA). The concentration of enzyme was 2.3 nM, and the orotate formation was monitored at 287 nm, an isosbestic point of Q_0. Application of the program of Cleland gave K_M values for DHO and Q_0 which were 27.5 ± 2.2 and 39.4 ± 3.8 μM, respectively. The V_{max} value obtained, 0.113 min^{-1}, corresponds to 215 μmol of orotate formed per min and mg of enzyme.

double reciprocal plot of reaction velocity versus substrate concentration (Figure 3). This initial velocity pattern indicates that DHOD from *E. coli*, like many other flavoenzymes, follows a Ping-Pong type of mechanism. Inhibition by the reaction product, orotate, was analyzed to further elucidate the mechanism. When the electron acceptor concentration was kept constant, the addition of orotate increased the apparent K_M values for DHO but left the apparent V_{max} values unaffected (Figure 4). This shows that orotate is a competitive inhibitor ($K_{is} = 13.4 \pm 0.8$ μM) with respect to DHO. It indicates that there is no competition between orotate and the electron acceptor, because such a competition would have caused reduction of the apparent V_{max} values in the presence of orotate (a K_{ii} value of $\approx 1 \times 10^{25}$ μM was obtained). In a complementary experiment, we observed uncompetitive inhibition between orotate and the electron acceptor DCIP in the presence of a constant concentration of DHO (200 μM). Parallel lines were obtained in the double reciprocal plot (not shown), and the variation of the intercepts on the ordinate indicated an apparent K_{ii} value of 148 ± 20 μM for orotate ($K_{is} \approx 1 \times 10^{15}$ μM), which is in agreement with the parameters obtained in the experiment shown in Figure 4. These results indicate strongly that the *E. coli* DHOD works by a two-site Ping Pong mechanism with one binding site for DHO and orotate and a different binding site for reduced and oxidized electron acceptor. Both the bovine liver and the mouse enzyme (from L1210 cells) have earlier been shown to operate by similar mechanisms (*12*, *13*), but, in contrast, DHODA, which belongs to the family 1 DHODs, appears to use one binding site for both DHO and electron acceptor (*1*).

In contrast to the sequential mechanisms, the Ping-Pong mechanisms are supposed to catalyze exchange reactions. The exchange of reducing equivalents (hydrogen atoms) between DHO and orotate was detected as transfer of the radioactive label from ^{14}C-labeled orotate to DHO, which migrates more quickly than orotate by chromatography on

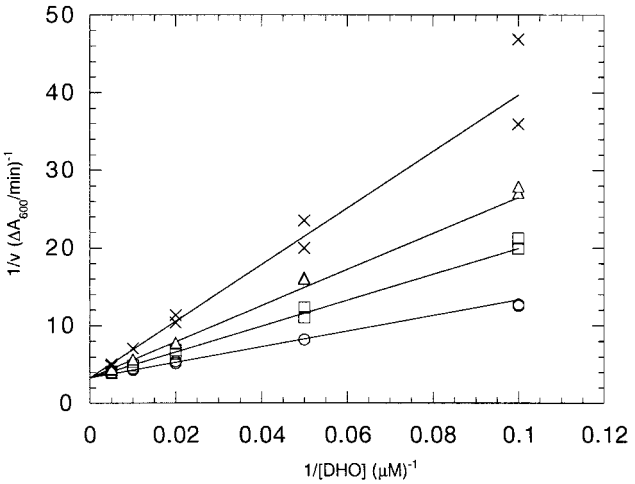

FIGURE 4: Inhibition of *E. coli* DHOD by orotate. The effect of orotate, 0 μM (circles), 10 μM (squares), 20 μM (triangles), 40 μM (crosses), while varying the concentration of DHO (10, 20, 50, 100, and 200 μM) is displayed by a double reciprocal plot. The experiment was carried out in standard buffer using the mixed electron acceptor system 200 μM Q_0 and 45 μM DCIP. As shown, the presence of orotate affected only the slopes and not the intercepts on the *y*-axis. Application of the program of Cleland, assuming noncompetitive inhibition, gave a K_{is} value of 13.4 $\pm$ 0.8 μM (and a K_{ii} value of $\approx 2 \times 10^{25}$) for orotate and a K_M value of 28.8 $\pm$ 1.5 μM for DHO. The V_{max} value obtained, 0.3054 $\pm$ 0.004 min^{-1}, corresponds to 180 μmol of DCIP reduced per min and mg of protein.

the PEI plates. The exchange reaction was studied under semianaerobic conditions (as described in Materials and Methods) to minimize the loss of electrons to oxygen. From two reactions, with 2 and 4 μM concentrations of enzyme, respectively, the initial rate of the exchange reaction was estimated to be about 0.13 μmol min^{-1} mg^{-1} and, thus, much lower than the rate of the steady-state reactions with other electron acceptors. Apparently, the reduced enzyme has a very poor ability to use orotate as electron acceptor, meaning that the first half-reaction is essentially irreversible for *E. coli* DHOD. However, the DHODA from *L. lactis* catalyzed a much more rapid exchange reaction (17 μmol min^{-1} mg^{-1}), comparable to the rate of steady-state reactions with other electron acceptors.

Preference for Electron Acceptors. A comparison of the activities of *E. coli* DHOD and DHODA in the presence of different electron acceptors was made (Table 1). Detergent (0.1% reduced Triton X-100) was included in the assays, which were performed at 25 °C because DHODA appeared unstable at 37 °C with molecular oxygen as electron acceptor. The concentrations of electron acceptor employed, 20 μM for the quinones and for DCIP and 500 μM for fumarate, were not saturating, implying that the reaction rates reported in Table 1 reflect a mixture of affinity and catalytic rate. Because the conditions were aerobic, there was always a residual activity with O_2 if no usable electron acceptor was present. It appeared that the reactivity with molecular oxygen was much stronger for DHODA than for the *E. coli* enzyme (Table 1).

The quinone, Q_0, appeared to be an almost equally good electron acceptor for the two enzymes, both with respect to K_M and V_{max}. These parameters were 40 μM and 215 μmol min^{-1} mg^{-1} for the *E. coli* enzyme (Figure 3) and were recently found to be 75 μM and 200 μmol min^{-1} mg^{-1} for

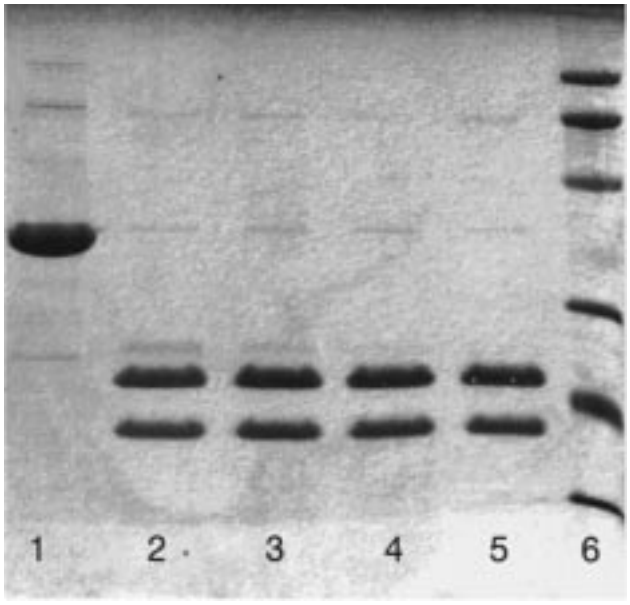

FIGURE 5: SDS−PAGE of trypsin-digested DHOD. Lane 1: undigested enzyme. Lanes 2−5: enzyme digested with trypsin. The concentration of trypsin was 200, 100, 50, and 10 μg/mL, in lanes 2, 3, 4, and 5, respectively. The marker proteins in the last lane (lane 6) are 97, 66, 45, 31, 21, and 14 kDa.

DHODA (*1*). A distinctive feature between the two enzymes is that only DHODA can use fumarate as electron acceptor, while only the *E. coli* enzyme can use decylubiquinone (Table 1). The reaction with decylubiquinone, the fastest one observed, did not occur without the presence of detergent, which probably contributes to the solubility of the substrate. The presence of detergent also improved the reactivity of *E. coli* DHOD with DCIP (about 2-fold). The other rates shown in Table 1 were not greatly influenced by detergent.

Determination of the Trypsin Cleavage Site. By coincidence, we discovered that native *E. coli* DHOD was very susceptible to cleavage by trypsin. Concomitant with loss of activity, the 37 kDa enzyme was degraded and two large fragments of 22 and 18 kDa appeared on SDS−PAGE. The cleavage reaction was very specific, and increasing the concentration of trypsin from 10 to 200 μg/mL did not result in further fragmentation (Figure 5, lanes 2−5). This is a surprising result since *E. coli* DHOD contains many potential cleavage sites, 21 lysine and 17 arginine residues. However, when the concentration of trypsin was higher (1000 μg/mL) than that of DHOD (600 μg/mL), a degradation into low molecular weight fragments, not resolved by SDS gel, was evident. When the concentration of trypsin was low (0.5 μg/mL), the presence of 1 mM orotate protected the enzyme from digestion. The half-life of activity then increased from 20 min to 2 h (data not shown). Under native conditions, the two fragments obtained by limited proteolysis (10 μg trypsin/mL) remained associated with each other since there was no change in the mobility by chromatography on a gel filtration column or by electrophoresis in a native polyacrylamide gel.

The two fragments from the SDS gel were transferred to a PVDF membrane by electroblotting and subjected to automatic Edman degradation. The N-terminal sequence of the larger fragment was MYYPFVXKAL, corresponding to the N-terminus of the undigested enzyme (where X is R). For the smaller fragment, the sequence TLQYGEALDD was

obtained and it corresponds to residues 183−192 in the undigested enzyme. A cleavage site at the position of R182 was thus identified. The cleavage site is located in a region which is conserved between the two major families of DHODs (see Figure 1 and Discussion). If the enzyme was cleaved exclusively at this position, the predicted masses of the two fragments would be 20 103.2 Da (for residues 1−182) and 16 689.3 Da for (residues 183−336), according to the protein sequence. The C-terminal ends of the two fragments isolated by SDS−PAGE were not analyzed. We reasoned that secondary cleavages would be revealed by MALDI MS analysis, because cutting at the closest potential site in the large fragment (K161) would reduce the mass by 2098 Da, and cleavage at K330 would reduce the mass of the smaller fragment considerably and release a hexapeptide with a mass of 711 Da.

The expected mass of the undigested enzyme is 36 774 Da according to the protein sequence. Several independent measurements by MALDI MS of the mass of the native enzyme resulted in determinations varying between 36 800 and 36 808 Da. The peaks exhibited tailing toward higher mass, indicative of partial oxidation of methionine residues and/or salt and matrix adducting. Oxidation of methionine is a frequently observed artifact during sample preparation for MALDI MS. The sample appeared free from other contaminating proteins since all peaks in the spectra could be attributed to different charged states or multimers of the enzyme. Analysis by MALDI MS of the enzyme after tryptic digestion revealed two new major peaks. The first peak indicated the presence of a peptide with mass 20 137 Da, corresponding to the fragment containing residues 1−182, assuming partial oxidation of the five methionine residues in this peptide. The second peak was split, indicating the presence of two components, one with a mass of 16 704 Da and the other with a mass of 16 778 Da. The first component corresponds to the peptide containing residues 183−336, assuming an average of one methionine residue oxidized in this peptide which contains two methionine residues. It is unclear if the second component is caused by adduct ion formation to the peptide 183−336 or represents an additional loss of a peptide from the large peptide (1−182). That additional degradation of the two large peptides takes place, although at a low extent, is supported by the presence of a number of minor peaks in the mass range up to 12 000 Da, including one at 3437 Da corresponding to the peptide 1−27. At higher mass range, two small peaks were observed: one at 23 369 Da, interpreted as trypsin, and another one at 36 901 Da, within the range of undigested enzyme. In conclusion, the analysis suggested that the enzyme was predominantly cleaved by trypsin in a single position (R182), as it also appeared from the SDS gel (Figure 5).

Spectral Properties of Wild-Type and Modified Enzyme. Absorption spectra of the wild-type and cleaved enzyme, as well as two mutant forms of the protein, S175A and S175C (described below), were very similar. As judged from the release of free FMN, the extinction coefficients at 456 nm were about 13 500 ± 500 M^{-1} cm^{-1}. Thus, interactions with the enzymes both produce a red-shift of the spectrum and enhance the absorbance of the bound FMN, relative to free FMN. These interactions are also responsible for a strong quenching of the fluorescence of the bound FMN, as shown in Figure 6. The *L. lactis* DHODA gave 15 times less

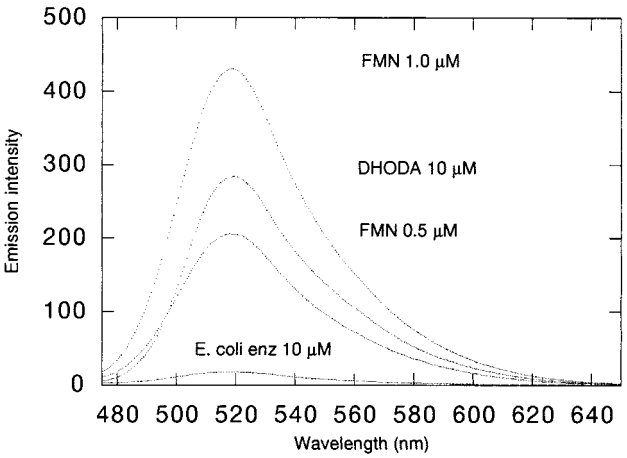

FIGURE 6: Fluorescence emission spectra of FMN bound to *E. coli* DHOD and *L. lactis* DHOD. The enzymes were dissolved in 0.1 M Tris−HCl, pH 8.0, to 10 μM. The spectra were recorded with a Perkin-Elmer LS-50B luminescence spectrometer with an excitation wavelength of 450 nm. Slit widths for the monochromators of 5 nm and a scan speed of 50 nm/min were employed. As a comparison, the emission of free FMN, 1.0 and 0.5 μM, was recorded under the same conditions. Expressed on a molar basis, the fluorescence intensity at 520 nm of free FMN was 210-fold stronger than that of *E. coli* DHOD and 15-fold stronger than that of *L. lactis* DHOD.

fluorescence than free FMN, and, in turn, the *E. coli* enzyme gave 15 times less fluorescence than DHODA. The strong quenching of the FMN fluorescence was retained by the *E. coli* DHOD, even after digestion with trypsin or introduction of the two mutations, S175A and S175C.

Upon addition of orotate, the flavin absorbance of wild-type *E. coli* DHOD displayed a prominent red-shift, as the main peak of absorbance was moved from 456 to 475 nm. This phenomenon was observed by Larsen and Jensen (*15*) but not interpreted. The difference in absorption between the red-shifted enzyme and the initial spectrum was largest around 515 nm, because there was essentially no absorbance at this wavelength before the addition of orotate. The size of the red-shift showed saturation with increasing concentration of orotate and could be used to estimate the binding parameter for orotate, as described for the *L. lactis* enzyme (*1*). We obtained a K_D value of about 5 μM for the wild-type enzyme, while the K_D was increased to 20 μM for the trypsin-cleaved enzyme (Figure 7). The S175C mutant also showed a reduced affinity for orotate ($K_D = 10.8 \pm 1.1$ μM), but the S175A mutant appeared to be normal in this respect ($K_D = 6.4 \pm 1.0$ μM).

Activity of the Trypsin-Digested Enzyme. After treatment with trypsin, about 0.5% of the initial activity remained in the digested samples. A higher concentration of trypsin (up to 400 μg/mL) did not affect this level of residual activity, nor did the addition of Triton X-100 during digestion. We examined the kinetic parameters of the remaining enzyme activity. The K_M values for DHO and the inhibitor constant (K_{is}) for orotate were 28.0 ± 1.0 μM and 11.1 ± 0.5 μM, respectively, not significantly different from the corresponding parameters for the intact protein, but a lower K_M value, 14.6 ±1.8 μM, for DCIP was observed, compared to 30.2 ± 2.2 μM for undigested enzyme. The relative level of residual activity was the same, about 0.5%, with the mixed electron acceptor system or with Q_0, DCIP, decylubiquinone, or menadione used alone as electron acceptors. The level

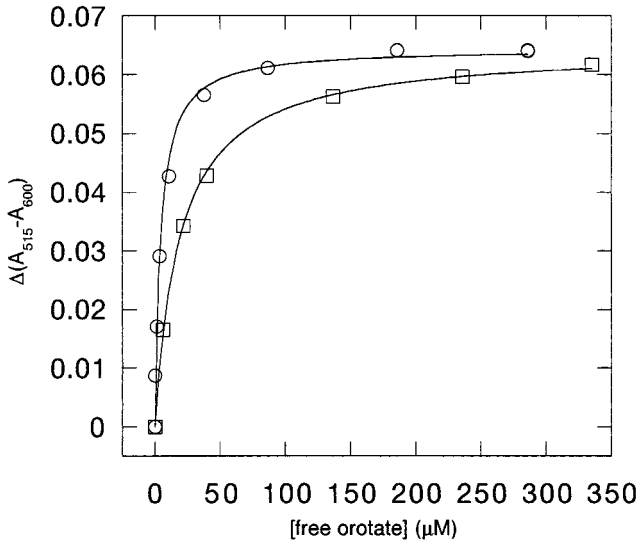

FIGURE 7: Binding of orotate to uncleaved and cleaved DHOD. Wild-type DHOD was diluted in 0.1 M Tris−HCl, pH 8.0, and 200 μM PMSF, centrifuged, and transferred to the cuvette. The initial enzyme concentration (15 μM) was determined from the absorbance at 456 nm. Spectra were then recorded after eight successive additions of orotate, and the resulting red-shift of flavin absorbance, $\Delta(A_{515} - A_{600})$, was analyzed as described in Materials and Methods. The resulting curve (circles) indicates an apparent dissociation constant of 4.4 ± 0.7 μM. The next saturation curve (squares) was obtained with DHOD digested with trypsin. The enzyme was diluted in 0.1 M Tris−HCl, pH 8.0, including trypsin (10 μg/mL). After 20 min at room temperature, PMSF was added to 200 μM and the sample was centrifuged. Spectra were recorded to determine the enzyme concentration (16 μM) and to follow the absorbance changes resulting from six additions of orotate. The apparent dissociation constant for enzyme digested by trypsin was 19.3 ± 0.7 μM.

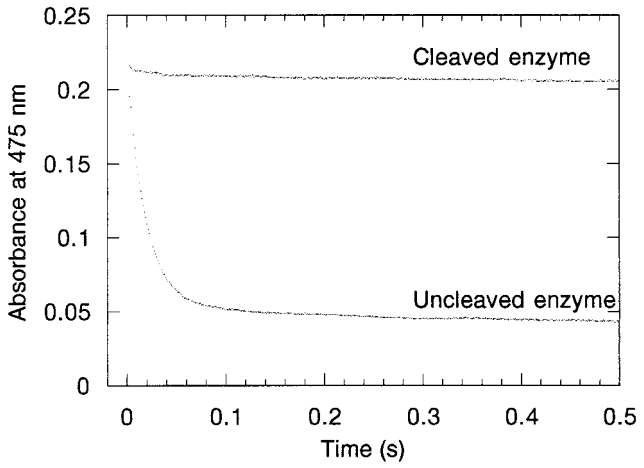

FIGURE 8: Reduction of uncleaved and cleaved enzyme by DHO. Enzyme and substrate were diluted in 0.1 M sodium phosphate, pH 7.0, 0.1 mM EDTA containing 5 mM glucose, and glucose oxidase (0.04 mg/mL) in order to reduce the reoxidation of the flavin cofactor by molecular oxygen. In the stopped-flow apparatus, enzyme and DHO were mixed at 25 °C (1:1) to final concentrations of 18 μM and 1 mM, respectively. After 200 s, the absorbance of the cleaved enzyme had decreased to 0.15.

was also constant in the pH range 6.0−9.0 (measured with Q_0 as electron acceptor). A very slow and incomplete bleaching was observed in a stopped-flow experiment (Figure 8), demonstrating that the cleaved enzyme is severely defective with respect to the first half-reaction. In contrast, ligand binding does not seem to be much damaged because the cleaved enzyme bound orotate reasonably well according to the red-shift of flavin absorbance (Figure 7) and because, furthermore, a red-shift of the flavin absorbance was observed upon binding of DHO, as also seen on intact enzyme (Dr. B. Palfey, unpublished observation).

It is possible that residual activity results from a protease-resistant form of the enzyme, because we observed a small amount of protein material left with the same mobility as the undigested enzyme on SDS gels, and a very minor peak at 36 901 Da was detected by MALDI MS. However, it is also possible that the cleaved enzyme is responsible for the residual activity. Attempts to blot and sequence the faint band remaining at 37 kDa were unsuccessful. Thus, we are unable to distinguish between the two explanations for the residual activity.

Activity of the S175 Mutant Enzymes. The change of cysteine 130 to alanine or serine in *L. lactis* DHODA reduced the activity by more than 5000-fold, to levels which were difficult to monitor in our assay system (*1*). According to the sequence alignment (Figure 1), a serine residue (S175) in *E. coli* DHOD has replaced the active site cysteine residue (C130) in DHODA. Therefore, we selected S175 in the *E. coli* enzyme for mutagenesis to alanine and cysteine, respectively. The S175A mutant displayed very little activity. The kinetic parameters could not be determined because the decrease in the specific activity was more than 10 000-fold. However, the S175C mutant enzyme had sufficient activity to allow some characterization. When employing the mixed electron acceptor system, the apparent V_{max} was decreased 500-fold relative to the wild-type enzyme. The apparent K_M value for DHO (92.9 ± 6.2 μM) was higher than for the wild-type enzyme, while the apparent K_M for DCIP (14.6 ± 1.6 μM, obtained in the presence of 1.0 mM DHO) was reduced 2-fold. The reduced K_M for DCIP is consistent with a catalytic block of the first half-reaction. The increased K_M for DHO suggests a binding defect since the alternative explanation, a great enhancement of the second half-reaction, seems unlikely. Thus, the substitution of serine 175 to cysteine affected both catalysis and binding of DHO. Weaker competitive inhibition by orotate (K_{is} = 51.2 ± 5.8 μM) was observed, and a lower affinity for orotate was also suggested from the red-shift of flavin absorbance (see above). Neither of the two S175 mutants was bleached by DHO, but the red-shift of flavin absorbance by DHO was observed.

Protein Stability. According to DSC, the *E. coli* enzyme was much more stable than the *L. lactis* DHODA ($t_m \approx 70$ and 50 °C, respectively, shown in Figure 9). The DSC scans could be fitted well to a non-two-state model of unfolding, but under the conditions used, the thermal transitions were not reversible when the samples were heated to 5 °C above the t_m (75 and 55 °C, respectively). The two mutant enzymes, S175A and S175C, retained the t_m of the wild-type protein, and, more interestingly, the t_m was also retained after digestion with trypsin (Figure 9). This result strongly suggests that the trypsin cleavage site, R182, is positioned in a loop, which is crucial for catalysis, but irrelevant for protein stability.

DISCUSSION

Our recombinant enzyme showed a strong tendency to high apparent molecular weight during gel filtration and

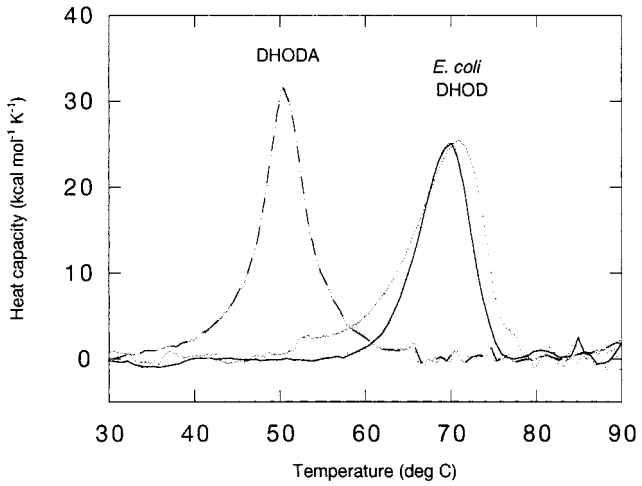

FIGURE 9: DSC scans comparing DHOD from *L. lactis* (DHODA) and *E. coli*. The scanning conditions are described in Material and Methods. The dotted curve represents *E. coli* DHOD digested with trypsin.

sedimentation in the sucrose gradients without detergent. In the presence of detergent, however, the migration in the sucrose gradient corresponded to a dimer (72 kDa), a result consistent with that of Karibean and Couchoud (*22*). These investigators found that the apparent size was proportional to the amount of loaded material on a gel filtration column and that extrapolation to zero protein concentration gave a molecular weight of 67 kDa. DHODA of *L. lactis*, which belongs to family 1, is also a dimer, both in solution (*3*) and in crystals (*9*). Dimer formation is probably necessary for protein stability since a large hydrophobic cavity is shielded in the subunit interface, but each of the two active sites is formed by residues from one subunit only. Therefore, dimer formation may not be an absolute requirement for activity. Although sequence identity is low between the two families of DHODs, it is likely that the overall fold is conserved, but it is not evident that a dimeric state, found here for the *E. coli* enzyme, is typical for all family 2 enzymes. A monomer form of recombinant human enzyme (42 kDa) was recently observed by Knecht et al. (*6*) using gel filtration in the presence of 1% octylglycoside. A higher apparent M_r of the human enzyme, 120 kDa, was observed by Copeland et al. (*23*), but their recombinant enzyme was N-terminally truncated, which may have affected the solubility properties. In earlier studies of the bovine liver enzyme, Hines et al. (*11*) observed a broad size distribution, 60−120 kDa, by glycerol gradient centrifugation in the presence of Triton X-100, and in gel-filtration experiments with Triton X-100, they found an apparent size of more than 200 kDa, although the subunit molecular weight of the bovine enzyme was 42 kDa.

Association to membranes is conceivably related to the use of respiratory quinones as electron acceptors. The *E. coli* enzyme could efficiently use the soluble analogue, decylubiquinone. This analogue was completely rejected by DHODA. The two DHODs were also fully differentiated with respect to fumarate, which was used only by DHODA. Differences in electron acceptor binding are also evident from the inhibition by orotate, which did not compete with binding of the electron acceptor in *E. coli* DHOD, indicating that this enzyme employs a two-site ping-pong kinetic mechanism, consistent with the very poor ability of reduced *E. coli* DHOD to transfer electrons to orotate, as shown by the slow DHO−orotate exchange reactions. Such two-site mechanisms are frequently seen for dehydrogenases with two or more flavins, for instance the dihydropyrimidine dehydrogenases (*24*), but are more difficult to envision for smaller enzymes such as the *E. coli* DHOD, which has only one flavin. According to the two-site model, the reducing equivalents in this enzyme would enter FMN from one site, which binds DHO, and leave FMN toward a nonoverlapping site, which binds the electron acceptors (the quinones). In contrast, the family 1 enzyme, DHODA from *L. lactis*, uses the same site for binding of both the substrate DHO and the electron acceptor (*1, 3*). The crystal structure of DHODA revealed that this binding site is located in a cavity above the isoalloxazine ring of the flavin and that the substrate/product (DHO/orotate) stacks tightly to the *si* side of the flavin during binding (*9, 10*). The marked red-shift of the flavin absorbance, seen after the binding of orotate, and the amino acid similarities between the two enzymes indicate that orotate/DHO also binds with close stacking to FMN in the *E. coli* enzyme, but the 3-dimensional structure of DHODA does not give any clue regarding the location of the quinone binding site in the family 2 enzymes. However, it is apparent that the DHODs belonging to family 2 have extensions of at least 40 amino acid residues in the N-terminal, where there is very little similarity between the mammalian enzymes and the enzymes from Gram-negative bacteria. There is no correspondence at all to DHODA and other family 1 enzymes (*2, 9*). In this region, Löffler and co-workers (*6*) have identified mitochondrial targeting sequences from the cDNA of rat liver and human DHOD and similar sequences were found for the DHOD of *Drosophila* (*25*). In contrast to the *E. coli* enzyme, the mammalian DHODs are extremely sensitive to Brequinar sodium and the Leflunomide metabolite, A771726, immunosupressive compounds which appear to interfere with electron acceptor binding (*6, 13, 14, 26*). Recently, Davis and Copeland isolated a Brequinar-resistant mutant in the human enzyme (*27*). The mutated residue (H26A) is positioned in the N-terminal region, implying an importance of this region for binding of the inhibitor. Thus, it is very tempting to speculate that the binding sites for the quinone acceptors are formed by the N-terminal extensions in the family 2 DHODs. Compared to DHODA, the *E. coli* enzyme is elongated by about 40 residues in the N-terminal end (*9*). The fact that very little cleavage by trypsin occurred in this region of the enzyme indicates that the N-terminal residues are part of the compact globular fold and may be important for enzyme function.

From a sequence alignment, it is evident that the *E. coli* enzyme is digested by trypsin in a region that is conserved between DHODs of both families 1 and 2 (Figure 1 and ref *9*). In DHODA, the residues 129−137 form a flexible loop which connects a β-strand (β4) and an α-helix (αA). The loop encloses a cavity identified as the substrate binding site. Upon binding of the reaction product, orotate, the loop loses flexibility and three fixed water molecules are expelled from the cavity. Stacking of the planar orotate molecule to the isoalloxazine ring as well as numerous H-bonds to enzyme residues all seem to contribute to binding. Some of the residues involved in H-bonding are completely conserved across families 1 and 2, and four Asn residues (N67, N127, N132, and N193), scattered over the sequence, particularly attract our attention. The side chains of N67 and N193 both

form bidentate interactions to orotate, and N132 is situated in the flexible loop. The conservation of the four Asn residues suggests that DHO−orotate binding can be accomplished very similarly in the family 2 enzymes. However, in the setup of catalytic residues around DHO−orotate there is at least one important difference, since in DHODA, we have identified a cysteine residue (C130) in the active site loop as being very critical for catalysis. The cysteine was suggested to function as a catalytic base, which abstracts a proton from the 5-position of dihydroorotate to facilitate transfer of a hydride ion from DHO to FMN. From sequence alignments, it appears that the cysteine residue has been replaced by a serine residue in all family 2 enzymes (Figure 1). We found that the substitution of serine 175 in the *E. coli* enzyme by alanine reduced the activity by a factor of 10 000, a result analogous to that observed for DHODA in the corresponding replacement (C130A). It is likely that serine175 in the *E. coli* enzyme plays the same mechanistic role as Cys 130 in DHODA.

A serine residue is less reactive as a base than cysteine, but it is also much less sensitive to reactive oxygen species. The reoxidation of a DHOD by molecular oxygen generates H_2O_2 which, appearing in the active site, is very harmful to a cysteine residue. DHODA, but not *E. coli* DHOD, is easily inactivated by H_2O_2 (data not shown). Mutagenesis of serine 175 in *E. coli* DHOD to cysteine gave a strong catalytic defect, a 500-fold reduction of the apparent V_{max}. The amino acid substitution also decreased the affinity for the substrate, DHO, and the product, orotate, indicating that serine 175 is also involved in substrate binding. In the work carried out on DHODA, the catalytic defects of the C130S mutant enzyme were very severe, but effects on substrate binding were not observed. The structure of DHODA in complex with orotate shows only minor hydrophobic contact between Cys 130 and the planar orotate molecule. However, the substrate, DHO, is not aromatic like orotate. Modeling of the substrate in the active site suggests that its carboxylate group gets in close contact with Cys 130 (*10*). The substrate itself could therefore increase the base character of the cysteine residue by acting as a transient acceptor of a proton. This could be true also for the family 2 enzymes, such as *E. coli* DHOD, which have serine in the active site. Being a weaker base than a cysteine residue, a serine residue would be more dependent on the local environment. However, a substrate-assisted catalysis involving the carboxylate group of DHO is not consistent with the results of Hines and Johnston, who investigated the activity of the bovine liver enzyme with esters of DHO (*11*, *12*). They found that the esters (methyl, ethyl, *tert*-butyl, and benzyl esters of DHO) were good substrates for that enzyme. Apparent V_{max} values were similar to that observed for (unsubstituted) DHO, while the apparent K_M values were elevated. According to these results, a free C-6 carboxylate anion seems not to be necessary for the enzymatic reaction. Furthermore, surprisingly large substitutions were tolerated by the enzyme. Because it was not clear how the stability of the esters in water solutions were accounted for, we have started to reinvestigate DHO esters as possible substrates of the DHODs. Our preliminary results with the methyl ester suggest that all observed activity can be attributed to a rapid hydrolysis of the compound (O. Björnberg, unpublished observations). Thus, the complete elucidation of the reaction mechanisms of the DHODs requires much further experimentation, most of it conducted under anaerobic conditions.

ACKNOWLEDGMENT

We thank Dr. Bent Sigurskjold, Department of Biochemistry, August Krogh Institute, University of Copenhagen, for help with interpreting the DSC data, and Dr. Bruce A. Palfey, University of Michigan, Ann Arbor, for communicating unpublished information. Nette Larsen is thanked for excellent technical assistance.

REFERENCES

1. Björnberg, O., Rowland, P., Larsen, S., and Jensen, K. F. (1997) *Biochemistry 36*, 16197−16205.
2. Jensen, K. F., Björnberg, O., Rowland, P., and Larsen, S. (1998) *Paths pyrimidines 6*, 20−28.
3. Nielsen, F. S., Rowland, P., Larsen, S., and Jensen, K. F. (1996) *Protein Sci. 5*, 857−861.
4. Nielsen, F. S., Andersen, P. S., and Jensen, K. F. (1996) *J. Biol. Chem. 271*, 29359−29365.
5. Nagy, M., Lacroute, F., and Thomas, D. (1992) *Proc. Natl. Acad. Sci. U.S.A. 89*, 8966−8970.
6. Knecht, W., Bergjohann, U., Gonski, S., Kirschbaum, B., and Löffler, M. (1996) *Eur. J. Biochem. 240*, 292−301.
7. Karibian, D. (1978) *Methods Enzymol. 51*, 58−63.
8. Andersen, P. S., Jansen, P. J. G., and Hammer, K. (1994) *J. Bacteriol. 176*, 3975−3982.
9. Rowland, P., Nielsen, F. S., Jensen, K. F., and Larsen, S. (1997) *Structure 5*, 239−250.
10. Rowland, P., Björnberg, O., Jensen, K. F., and Larsen, S. (1998) *Protein Sci. 7*, 1269−1279.
11. Hines, V., Keys, L. D., III, and Johnston, M. (1986) *J. Biol. Chem. 261*, 11386−11392.
12. Hines, V., and Johnston, M. (1989) *Biochemistry 28*, 1222−1226.
13. Chen, S.-F., Perrella, F. W., Behrens, D. L., and Papp, L. M. (1992) *Cancer Res. 52*, 3521−3527.
14. Davis, J. P., Cain, G. A., Pitts, W. J., Magolda, R. L., and Copeland, R. A. (1996) *Biochemistry 35*, 1270−1273.
15. Larsen, J. N., and Jensen, K. F. (1985) *Eur. J. Biochem. 151*, 59−65.
16. Poulsen, P., Jensen, K. F., Valentin-Hansen, P., Carlsson, P., and Lundberg, L. G. (1983) *Eur. J. Biochem. 135*, 223−229.
17. Randerath, K., and Randerath, E. (1967) *Methods Enzymol. 12A*, 323−347.
18. Sanger, F., Nicklen, S., and Coulson, A. R. (1977) *Proc. Natl. Acad. Sci. U.S.A. 74*, 5463−5467.
19. Matsudaira, P. (1990) *Methods Enzymol. 182*, 602−606.
20. Martin, R. G., and Ames, B. N. (1961) *J. Biol. Chem. 236*, 1372−1379.
21. Cleland, W. W. (1979) *Methods Enzymol. 63*, 103−138.
22. Karibean, D., and Couchoud, P. (1974) *Biochim. Biophys. Acta 364*, 218−232.
23. Copeland, R. A., Davis, J. P., Dowling, R. L., Lombardo, D., Murphy, K. B., and Patterson, T. A. (1995) *Arch. Biochem. Biophys. 323*, 79−86.
24. Podschun, B., Cook, P. F., and Schnackerz, K. D. (1990) *J. Biol. Chem. 265*, 12966−12972.
25. Rawls, J., Kirkpatrick, R., and Lacy, L. (1993) *Gene 124*, 191−197.
26. Bader, B., Knecht, W., Fries, M., and Löffler, M. (1998) *Protein Expression Purif. 13*, 414−422.
27. Davis, J. P., and Copeland, R. A. (1997) *Biochem. Pharmacol. 54*, 459−465.

BI982352C